Anal Bioanal Chem (2012) 403:1577–1584
DOI 10.1007/s00216-012-5964-0

ORIGINAL PAPER

Substrate-dependent kinetics in tyrosinase-based biosensing: amperometry vs. spectrophotometry

Liza Rassaei · Jin Cui · Edgar D. Goluch · Serge G. Lemay

Received: 16 February 2012 / Accepted: 21 March 2012 / Published online: 25 April 2012

Abstract Despite the broad use of enzymes in electroanalytical biosensors, the influence of enzyme kinetics on the function of prototype sensors is often overlooked or neglected. In the present study, we employ amperometry as an alternative or complementary method to study the kinetics of tyrosinase, whose catalytic activity results in *o*-quinone products. We further compare our results for four monophenolic substrates with those obtained from ultraviolet–visible spectrophotometry and show that the results from both assays are in good agreement. We also observe large variations in the enzyme kinetics for different monophenolic substrates depending on the *R*-group at the *para* position. To further study this effect, we investigate the stability of quinone products in the enzymatic assay. This information can in principle be utilized to discriminate between different phenolic species by monitoring the reaction rate.

Keywords Voltammetry · Biosensor · Amperometry · Electroanalysis · Tyrosinase · Phenols · Quinones stability · Diffusion · Michaelis–Menten kinetics · Turnover rate · Microelectrode

L. Rassaei · J. Cui · S. G. Lemay (✉)
MESA+ Institute for Nanotechnology, University of Twente,
7500 AE Enschede, The Netherlands
e-mail: s.g.lemay@utwente.nl

E. D. Goluch · S. G. Lemay
Kavli Institute of Nanoscience, Department of Bionanoscience,
Delft University of Technology,
2628 CJ Delft, The Netherlands

Present Address:
E. D. Goluch
Department of Chemical Engineering, Northeastern University,
Boston, MA 02115, USA

Introduction

Enzymes are common recognition elements in electrochemical biosensors due to their high specificity, and the response of such sensors is therefore largely dictated by enzyme kinetics. A variety of methods such as radiometry [1], ultraviolet–visible (UV-Vis) spectrophotometry [2], manometry [3], and electrospray ionization with ion trap mass spectrometry [4] has been developed to study enzyme kinetics, with UV-Vis spectrophotometry being the most commonly employed as it is non-invasive, sensitive, inexpensive and allows the enzymatic reactions to be monitored continuously.

Tyrosinase is a copper containing protein that is able to bind dioxygen and catalyze the *ortho* hydroxylation of monophenols to *o*-diphenols (monooxygenase activity) and the oxidation of *o*-diphenols to the corresponding *o*-quinones (catechol oxidase activity) according to the following reaction:

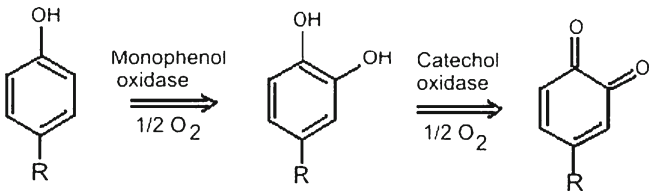

The binuclear copper center in the active site of tyrosinase exists in three different oxidation states depending on the copper ion valence and ability to bind with molecular oxygen: $Ty_{met}(Cu^{II}–Cu^{II})$, Ty_{oxy} $(Cu^{II}–O_2–Cu^{II})$, and $Ty_{deoxy}(Cu^{I}–Cu^{I})$ [5]. About 85 % of the enzyme in a fresh preparation at atmospheric pressure, room temperature, neutral pH and in the absence of substrate is in the *met* form with some variation depending on the source of the enzyme [6]. In this state, the

active site is in the bicupric form and unable to bind oxygen. Thus, only a small fraction of the enzyme is present in the *oxy* form [6]. The *oxy* form of tyrosinase can catalyze both the monooxygenase and catechol oxidase reactions, whereas the *met* form lacks the monooxygenase activity. Activation from the Ty_{met} form to Ty_{oxy} form takes place through the reaction of the enzyme with diphenols. Thereafter, Ty_{oxy} can react with monophenols to produce the *o*-quinones through diphenol intermediates. It is known that the catecholase activity of the enzyme is much faster [7, 8], thus the rate of conversion of phenol to quinone is limited by the rate of the monophenolase activity. The *o*-quinones regenerate the *o*-diphenol in the medium, which in turn reacts with and activate the remaining enzyme in the *met* form. The transformation of the enzyme from *met* form to *oxy* form introduces a short delay at the start of its reaction with monophenols called the lag phase.

Phenolic compounds present in pesticides, petroleum, textile, and paper-based materials released to the environment from industrial processes pose health and environmental concern due to their high toxicity. Measurement of phenolic compounds is also important in medical diagnostics and food inspection. In the past, analysis was mostly based on the spectrophotometric [2] or chromatographic [9] approaches. Electrochemical detection of phenols is based on their electro-oxidation which requires high positive potentials. This process is very complex, resulting in deactivation of the electrode due to the formation of a passivation of polymeric film from electrogenerated phenoxy radicals [10]. There is an interest in biosensors based on the reaction of phenolic compounds with tyrosinase which would potentially be simpler to make, easier to use, and less costly to manufacture. Tyrosinase has broad substrate specificity toward phenols relevant for a wide range of applications [11]. The enzymatic reaction of phenols can be monitored by various electrochemical detection techniques, including detection of dioxygen consumption [12], direct reduction of generated *o*-quinone [13], and coupled mediated reduction of *o*-quinone [14]. Among these methods, amperometric detection of the biocatalytically generated *o*-quinones is most common.

Tyrosinase biosensors have been proposed with enzyme immobilized on the electrode surface using variety of techniques including entrapment in conductive polymers such as polyaniline [15] or in a sol-gel membranes [16], covalent binding on gold nanoparticles [17] or self-assembled monolayers [18], adsorption to carbon nanotubes [19] or to zeolite particles [20], and entrapment with chitosan [21]. Although immobilized tyrosinase on the electrode surface has been reported to result in increased enzyme stability and allows reusing the sensor for a few times [22], in several cases it introduces problems with mass transfer of the substrate to the enzyme [23]. A much simpler approach is to add free enzyme to the sample solution as suggested in the recent publication of Adamski et al. [24]. Their approach utilizes a 10 minute integration of the amperometric signal for reduction of quinones produced from different phenolic substrates. Here, we show that the signal is however highly dependent on the nature of the substrate, which makes it less straightforward to use the suggested protocol for measurement of phenolic compounds.

Although structural and mechanistic data of tyrosinase exist [25], they have, thus far, not been extensively utilized in the design of enzyme-based sensors. For example, the *R*-group of phenols influences the reaction rate of tyrosinase *via* two factors, namely, the electronegativity of the *R*-group and the steric hindrance caused by the size of this group. The reactivity of tyrosinase decreases upon a transition of the substituent in the *para* position of phenols from electron donating to electron withdrawing [26], and tyrosinase does not react with bulky phenols [27]. There are few studies on kinetics of tyrosinase for different phenolic substrates with alkyl groups side chain such as methyl- [28], ethyl- [29], and *tert*-butylphenol [30]. To complete the series with the type of *R*-group substitutions, we have measured the turnover rate of tyrosinase for methyl-, ethyl-, isopropyl-, and *tert*-butylphenol using both UV-Vis spectrophotometry and amperometry techniques and show that the two methods are in good agreement. We also find that the nature of the *R*-group at the *para* position of the substrate has a strong impact on the obtained response.

Experimental details

Chemical reagents

Chemicals were obtained commercially in analytical grade and used without further purification. Mushroom (Agaricus bisporus) tyrosinase (4,276 unit/mg) was purchased from Sigma-Aldrich in lyophilized powder form. The powder was dissolved into a stock concentration of 10 μM and stored at −80 °C. Phosphoric acid 85 %, 4-methyl phenol, 4-ethyl phenol, 4-isopropylphenol, 4-*tert*-butylphenol, and sodium hydroxide were obtained from Sigma-Aldrich. Stock solutions of the phenolic substrates were freshly prepared in 0.2 M sodium phosphate-buffered solutions (pH= 6.7) before each experiment. Deionized and filtered water of a resistivity not less than 18 MΩ cm was taken from a Milli-Q Advantage ultrapure water system.

Instrumentation

Electrochemical experiments were performed in a two-electrode cell system (reference and counter electrodes were short circuited together which was appropriate due to the low current levels) using a CHI832 potentiostat. The

working electrode was a carbon fiber ultramicroelectrode (radius of 6±1 μm) from BASi. A 3 M Ag/AgCl electrode (BASi, USA) was used as a reference electrode. UV-Vis absorption spectra were recorded using a Carry 50 spectrophotometer (Agilent Technology). All the experiments were carried out at room temperature (20±2 °C).

Methods and procedures

Procedure for UV-Vis spectrophotometry measurements Enzymatic assays were conducted using UV-Vis spectrophotometry with a scanning speed of 600 nm min^{-1} and an interval of 1 nm following the appearance of the products in the reaction medium. Varying substrate concentrations were used against a fixed concentration of 100 nM tyrosinase unless stated otherwise. Absorbance was recorded at a wavelength of 400 nm. Reference cuvettes contained all of the components except the substrate, with a final volume of 2 ml. The absorbance data were analyzed according to the Beer–Lambert equation.

Determination of diffusion coefficients The diffusion coefficients for different quinones were obtained for each substrate using cyclic voltammetry at a carbon fiber ultramicroelectrode (radius of 6±1 μm). The phenolic solutions were first oxidized thoroughly using a high concentration of tyrosinase (1 μM). The product was then detected by repetitive potential cycling until the current reached its maximum value. Assuming that all the phenol was converted to quinone by tyrosinase, the diffusion coefficient was calculated using the equation $I_{lim}=4nFDrc$, where I_{lim} is the limiting current, n is the number of electrons transferred per molecule diffusing to the electrode surface, F is the Faraday constant, D is the diffusion coefficient, r is the electrode radius, and c is the bulk concentration of redox active reagent [31].

Procedure for electrochemical measurements The substrates used in electrochemical assays were 4-methylphenol, 4-ethylphenol, 4-isopropylphenol, and 4-*tert*-butylphenol. Formation of the reaction product was monitored using the amperometry technique at −0.2 V vs. 3 M Ag/AgCl.

Analyzing of kinetic data The time-dependent velocity of the reaction, V, was calculated by differentiating the concentration of quinone product vs. time. The maximum value was then selected to determine V. Typically, this maximum velocity was obtained in the first few minutes of each experiment. The maximum velocity, V_{max}, and the Michaelis constant, K_m, were subsequently obtained by nonlinear least-squares fitting of V against [S] according to the Michaelis–Menten kinetics model, $V = \frac{V_m[S]}{[S]+K_m}$ [32].

Results and discussion

Study of enzyme kinetics: UV-Vis spectrophotometry vs. amperometry

Although the kinetics of tyrosinase have been mostly studied using spectrophotometry techniques [2], the application of the enzyme in biosensing usually focuses on electrochemical approaches. However, the electrochemical study of tyrosinase kinetics and its comparison and validation against spectrophotometric techniques have not been the subject of any specific study. Here, we compare these two methods and discuss the consequences of tyrosinase's complexity in designing electrochemical sensors for phenolic compounds.

The quinone product of tyrosinase reaction with phenolic compounds is both electrochemically and spectrophotochemically active. It is therefore possible to monitor and compare its production in the enzymatic assay over the course of a reaction using both techniques. In order to have a broad range of comparisons for these two techniques, the activity of mushroom tyrosinase for four different substrates (4-methylphenol, 4-ethylphenol, 4-isopropylphenol, and 4-*tert*-butylphenol) is explored. For UV-Vis spectrophotometry measurements, the appearance of the product (quinone) and its evolution to a chromatophoric compound is measured at a wavelength of 400 nm, where the quinone absorption is maximum. For electrochemical measurements, the response is based on the amperometric detection of the biocatalytically generated *o*-quinones. Figure 1 shows the data for both methods using 4-ethylphenol as an example.

Figure 1A shows the absorbance vs. time for different concentrations of 4-ethylquinone. For low substrate concentrations, the absorbance increases monotonically with time before leveling off on a time scale of minutes. At this point, the substrate has completely been depleted in the reaction medium and transformed into *o*-quinone and thus the absorbance no longer changes with time. The time it takes to reach to this transition point varies for different concentrations of the substrate. For example, for a concentration of 25 μM, this is obtained after two minutes whereas for a concentration of 500 μM, four minutes are required. The figure also shows that at high substrate concentrations, true steady state conditions are not achieved. In these cases, the absorbance instead reaches a maximum before decreasing again. The monophenol oxidase reaction also depends on the presence of oxygen in the environment. Therefore, at high concentrations, the amount of phenol converted is limited by the amount of oxygen available in the assay [33, 34]. This limits the highest analyte concentration that a tyrosinase biosensor can detect. Figure 1B shows the data for the maximum reaction rates of different concentrations of 4-ethylquinone produced in the enzymatic

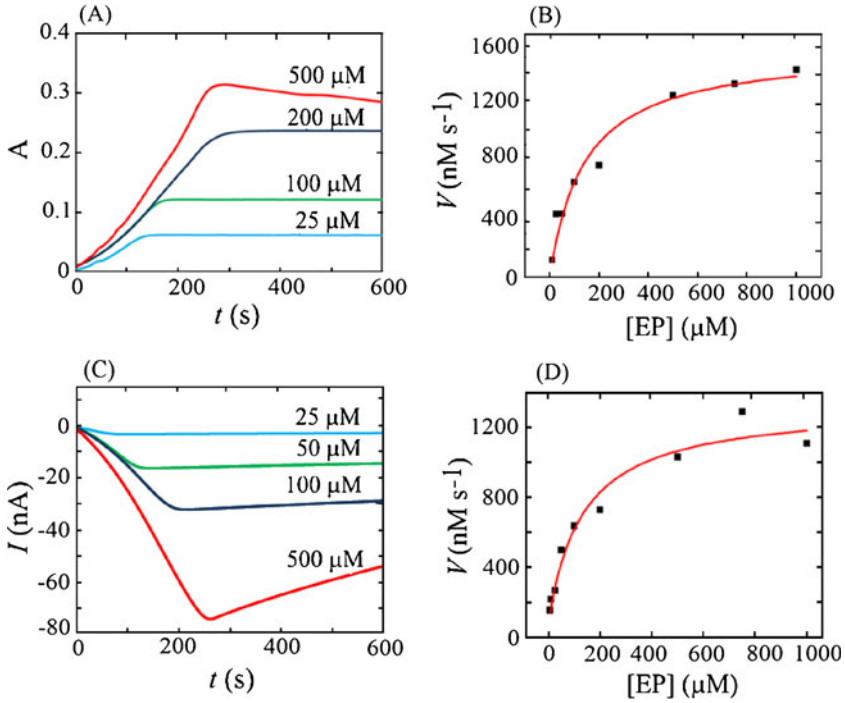

Fig. 1 (**A**) UV-Vis absorption (λ=400 nm) vs. time for different concentrations of 4-ethylphenol in 0.2 M phosphate buffer solution (pH=6.7) in the presence of 100 nM tyrosinase. (**B**) Plot of the reaction rate obtained from UV-Vis absorption vs. 4-ethylphenol concentration and fit to the Michaelis–Menten model. (**C**) Amperometry results (at a potential of −0.2 V) obtained for different concentrations of 4-ethylphenol under the same conditions as in (**A**). (**D**) Plot of the reaction rate obtained from amperometry results vs. 4-ethylphenol concentration and fit to the Michaelis–Menten model

assay vs. the substrate concentration. The reaction rate is approximately linear for the concentration range of 10 to 100 μM, above which it saturates to a maximum rate of 1.7 μM s^{-1}.

Tyrosinase has a complex kinetics associated with the lag phase at the beginning of its reaction and does not completely follow the common Michaelis–Menten model. Nevertheless for simplicity, we parameterize our data in terms of maximum velocity, V_{max}, and Michaelis constant, K_m. The red line in Fig. 1B shows the fit to this model. A turnover number of 17 s^{-1} per enzyme with a Michaelis constant of 130 μM was obtained for 4-ethylphenol for an enzyme concentration of 100 nM.

The final product of tyrosinase reaction with a monophenol is an *o*-quinone, which is electrochemically active and its reduction involves a two-electron process. The quinones can be reduced at the electrode surface when the required negative potential is applied according to the following reaction:

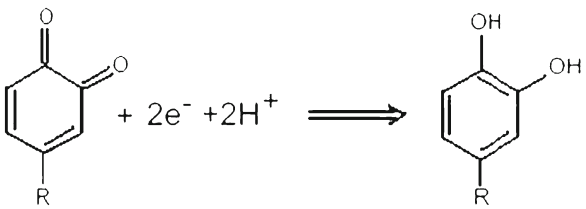

Ultramicroelectrodes, unlike macroelectrodes, have the advantage that they do not perturb the bulk reaction on experimental time scales. In particulare, due to the small size of the probe and spherical diffusion of material to the electrode, a time-dependent depletion zone of *o*-quinone does not establish itself at the electrode surface and the concentration of quinones in the bulk does not change significantly. The measured current is simply proportional to the concentration of quinones as they evolve in time, directly analogous to absorption in UV-Vis spectrophotometry. A carbon fiber ultramicroelectrode was used for this experiment. Experiments were carried out at a potential of -0.2 V vs. Ag/AgCl. Figure 1C shows the electrochemical responses for reduction of 4-ethylquinone for four different concentrations. A similar trend to those of spectrophotometry measurements was observed. For each concentration, the cathodic current for reduction of 4-ethyl quinone increased superlinearly, then reached a plateau where all the phenol was used up and converted to 4-ethylquinone. The time to reach the maximum current increased with the substrate concentration in a manner similar to what we observed using spectrophotometry.

At high concentrations, the faradaic currents for reduction of quinone did not reach a plateau, but declined after reaching a maximum point. In addition to oxygen depletion, as in the UV-Vis case, this may be influenced by the benzene derivative products which form oligomers among themselves, especially at high concentrations. The oligomers have much lower diffusion coefficients than the monomer and, thus, the transport to the electrode surface becomes more sluggish. The electron transfer rate may also be decreased as the electronic structure of oligomers differs from that of monomers.

Figure 1D shows the plot of the reaction rate for different concentrations of 4-ethylphenol and the fit to the Michaelis–Menten kinetics model. From this fit, a maximum rate of 1.4 μM s^{-1} and a Michaelis constant of 130 μM were obtained for an enzyme concentration of 100 nM, in good agreement with those of UV-Vis spectrophotometry.

Similar behavior was observed for both 4-methylphenol and 4-isopropylphenol, although longer times were required for the enzyme to convert 4-isopropylphenol to 4-isopropylquinone due to much lower turnover rates. This may be explained by the steric hindrance introduced via the isopropyl group at the *para* position. The results obtained for all four monophenolic substrates are summarized in Table 1 from which we can see that there is a good agreement between both techniques. The variation between the two methods are comparable to the uncertainty between measurements using the same technique. These data illustrate that the electronic structure of the substituent affects both the turnover rate of the enzyme and its affinity toward the substrate.

The reaction between tyrosinase and 4-*tert*-butylphenol differs from other substrates and in particular exhibits different kinetic behavior. Figure 2A shows the UV-Vis spectra for different concentrations of 4-*tert*-butylphenol. Due to the sluggish kinetics of tyrosinase for this substrate and limited resolution of our spectrophotometer, a higher concentration of tyrosinase (1 μM) was used in this experiment. For low concentrations of 4-*tert*-butylphenol, similar to the monophenols studied earlier, the absorption initially increases and then reaches a plateau; however, much longer periods of time are required to reach to this plateau. For example, for a concentration of 50 μM, this is achieved only after 13 min. For higher concentrations, this plateau is not established even after 30 min. Surprisingly, the rate at which the absorption changes decreased at higher substrate concentrations, as plotted in Fig. 2B. This is a different behavior from that of the other monophenols studied and is not consistent with the Michaelis–Menten kinetics model. This has been reported before by Ros et al. [30] and Fennol et al. [35], who related this behavior to both the suppressed autoactivation of tyrosinase from *met* to *oxy* form caused by binding of monophenols to the *met* form of the enzyme together with the high stability of quinone products.

The results from amperometry in this anomalous case are also in good agreement with those obtained from absorption spectra. Figure 2C shows the amperometry results obtained for different concentrations of 4-*tert*-butylphenol. The maximum reduction current for 4-*tert*-butylquinone increases with increasing of 4-*tert*-butylphenol concentration, while the reaction rate initially increases with 4-*tert*-butylphenol concentration and then declines, similar to the data obtained from spectrophotometry method (Fig. 2D). These studies complement earlier data and show the influence of the substituent side chain at the *para* position on the hydroxylating rate of monophenols. Phenols with a small substituent side chain, such as 4-ethylphenol and 4-methylphenol exhibit higher turnover rate. On the other hand, phenols with larger molecular size substituent side chain, 4-isopropylphenol and 4-*tert*-butylphenol exhibit much lower turnover rates.

For spectrophotometry measurements, the detection of quinone is limited by the resolution of the instrument. The main factor limiting the sensitivity of the amperometry method is instead the background current obtained in the absence of the analyte. The background current is mainly due to the presence of other electroactive substances such as oxygen. In this context, carbon electrodes have both the advantage of broader potential window when compared with the noble metals and that their catalytic activity toward the reduction of oxygen is poor.

Stability of *o*-quinones

Quinones are known to be unstable and undergo several non-enzymatic reactions [29, 35]. Here, we study the stability of the biocatalytic product of tyrosinase reaction with monophenolic substrates by following the evolution of their UV-Vis absorption spectra. The wavelength is scanned from 700 to 350 nm and the change in UV-Vis absorption spectra is recorded for 90 successive scans over 1.5 h.

Figure 3 shows a selection of the absorption spectra for evolution of *o*-quinones generated by oxidation of our four different monophenolic substrates using 500 nM mushroom tyrosinase. For 4-methylphenol (Fig. 3A), the absorption peak at 400 nm increases with the reaction time for the first

Table 1 A comparison of the results obtained from amperometry and UV-Vis absorption experiments and their fit to Michaelis–Menten kinetics model. The concentration of tyrosinase is 100 nM in all studies except for 4-*tert*-butylphenol where it is 1 μM

Substrate	UV-Vis		Amperometry	
	Turnover (s^{-1})	K_m (M)	Turnover (s^{-1})	K_m (M)
4-methylphenol	16	7×10^{-5}	24	2.1×10^{-4}
4-ethylphenol	17	1.4×10^{-4}	14	1.4×10^{-4}
4-isopropylphenol	1.5	1×10^{-4}	2.5	1.5×10^{-4}
4-*tert*-butylphenol	0.12	–	0.16	–

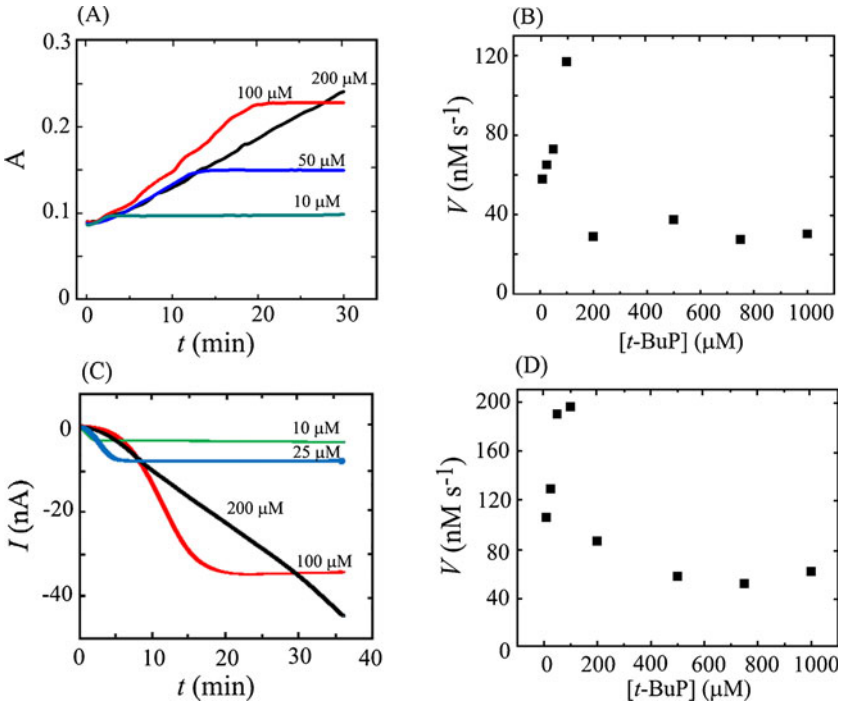

Fig. 2 (**A**) UV-Vis absorption (λ=400 nm) vs. time for different concentrations of 4-*tert*-butyl phenol in 0.2 M phosphate buffer solution (pH 6.7) in presence of 1 µM tyrosinase. (**B**) Plot of the reaction rate obtained from UV-Vis absorption vs. the 4-*tert*-butylphenol concentration. (**C**) Amperometry results (at potential of −0.2 V vs. Ag/AgCl) for different concentrations of 4-*tert*-butylphenol under the same conditions as in (**A**). (**D**) Plot of the reaction rate obtained from amperometry data vs. the 4-*tert*-butylphenol concentration

30 minutes with a maximum absorption of 0.29, then the absorption decreases for the next 10 min to 0.16. Finally, it gradually increases again to reach an absorption level similar to that of 30 min (0.29 at λ_{max}=400 nm) after 90 min. However, absorption at other wavelengths also slowly increases with time, especially around 500 nm. The progressive absorbance changes at other wavelengths can be attributed to the products from the nonenzymatic autopolymerization of *o*-quinones which yield several unstable intermediates, as reported previously [36, 37].

For 4-ethylphenol (Fig. 3B), the absorption increases gradually at 400 nm for the first 40 min with a maximum absorption at 0.26, then decays with time to 0.20. The absorption at other wavelengths (mainly at 500 nm) instead constantly increases with time. The absorption increase for 4-isopropylphenol (Fig. 3C) occurs for the first 60 min (A=0.37), after which it levels off and stops changing with time, whereas the absorption at 500 nm increases with time. Finally, Fig. 3D shows that the absorbance peaks (at 400 and 500 nm) from the product of oxidation of 4-*tert*-butylphenol

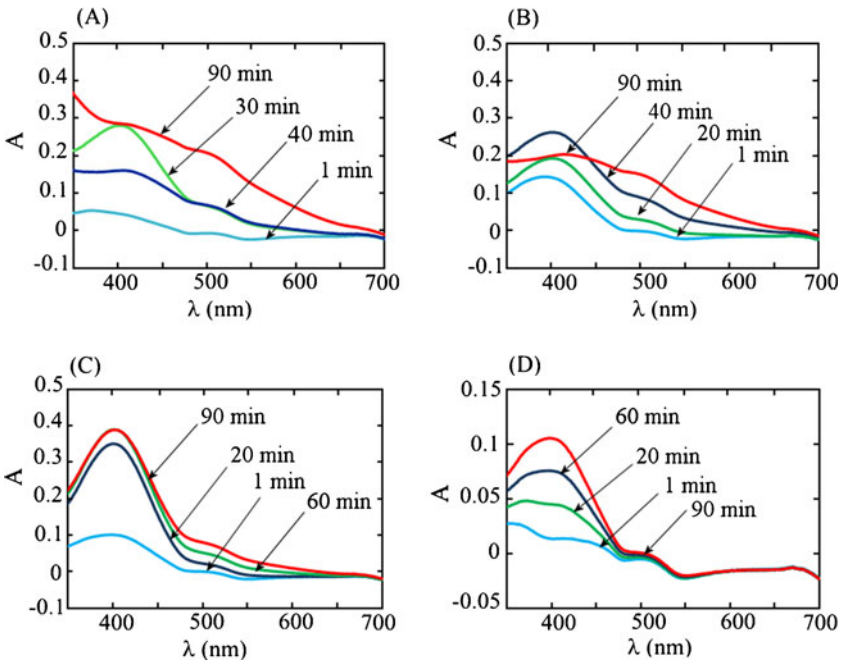

Fig. 3 UV-Vis absorption spectra for the evolution of *o*-quinones from the reaction of 500 µM of different monophenolic substrates (**A**) 4-methylphenol, (**B**) 4-ethylphenol, (**C**) 4-isopropylphenol, and (**D**) 4-*tert*-butylphenol with 500-nM mushroom tyrosinase for 90 min

increase with time and do not saturate even after 1.5 h. The contribution from the absorbance at 500 nm is insignificant compared with the other substrates studied here.

In all cases, the resulting *o*-quinones may undergo non-enzymatic autopolymerization to produce colored compounds which cause the red shift of the products and increase of absorbance at other wavelengths. The quinone produced in biocatalytic reaction can react with (1) water which acts as a weak nucleophile, (2) itself, or (3) the product resulting from adding water, and (4) the intermediate radicals formed in the enzymatic reactions. The products of the tyrosinase reaction with 4-methylphenol and 4-ethylphenol are unstable quinones that evolve very rapidly whereas they are more stable in the case of 4-isopropyl- and 4-*tert*-butylphenol. The following relative stability is thus suggested from Fig. 3:

$$-CH_3 < -CH_2(CH_3) < -CH(CH_3)_2 < -C(CH_3)_3$$

Importantly, different substrates have different time scales to reach the maximum absorbance where all phenols are expected to be converted to quinones. The trend here is exactly opposite to the one presented above for stability. Thus, the response time associated with the oxidation of the substrates by tyrosinase proves to be very sensitive to the nature of the substitutes present on the aromatic ring. The stability of the enzymatically generated *o*-quinones in the reaction medium is thus also an important parameter for designing a biosensor based on tyrosinase.

Conclusions

Amperometry was shown to be a rapid and sensitive continuous method for analysis of enzyme kinetics where the change in current for oxidation or reduction of substrate or product is followed vs. time at a suitably fixed biased potential. The kinetic mechanism of tyrosinase on different monophenolic substrates is very complex and dependent on the substituent group at the *para* position. This influences the measurement time for different monophenolic substrates and therefore, reliable calibration methods are a prerequisite for its application in biosensors.

Acknowledgments We gratefully acknowledge the financial support from the Netherlands Organization for Scientific Research (NWO) and the European Research Council (ERC). E. D. G. thanks the NSF for support through award #0754396.

References

1. Poland AP, Nebert DW (1973) A sensitive radiometric assay of aminopyrine *N*-demethylation. J Pharmacol Exp Ther 184:269–277
2. Garcia-Molina F, Munoz JL, Varon R, Rodriguez-Lopez JN, Garcia-Canovas F, Tudela J (2007) A review on spectrophotometric methods for measuring the monophenolase and diphenolase activities of tyrosinase. J Agr Food Chem 55:9739–9749
3. Gibson QH, Swoboda BE, Massey V (1964) Kinetics and mechanism of action of glucose oxidase. J Biol Chem 239:3927–3934
4. Ge X, Sirich TL, Beyer MK, Desaire H, Leary JA (2001) A strategy for the determination of enzyme kinetics using electrospray ionization with an ion trap mass spectrometer. Anal Chem 73:5078–5082
5. Aj S, Mason HS (1973) Magnetic dipole–dipole coupled Cu(Ii) pairs in nitric oxide-treated tyrosinase—structural relationship between active-sites of tyrosinase and hemocyanin. Proc Natl Acad Sci USA 70:993–996
6. Naish-Byfield S, Riley PA (1992) Oxidation of monohydric phenol substrates by tyrosinase. An oximetric study. Biochem J 288:63–67
7. Ben-Yosef VS, Sendovski M, Fishman A (2010) Directed evolution of tyrosinase for enhanced monophenolase/diphenolase activity ratio. Enzyme Microb Technol 47:372–376
8. Hernandez-Romero D, Sanchez-Amat A, Solano F (2006) A tyrosinase with an abnormally high tyrosine hydroxylase/dopa oxidase ratio—role of the seventh histidine and accessibility to the active site. FEBS J 273:257–270
9. Heberer T, Stan HJ (1997) Detection of more than 50 substituted phenols as their t-butyldimethylsilyl derivatives using gas chromatography mass spectrometry. Anal Chim Acta 341:21–34
10. Iotov PI, Kalcheva SV (1998) Mechanistic approach to the oxidation of phenol at a platinum/gold electrode in an acid medium. J Electroanal Chem 442:19–26
11. Duran N, Rosa MA, D'Annibale A, Gianfreda L (2002) Applications of laccases and tyrosinases (phenoloxidases) immobilized on different supports: a review. Enzyme Microb Technol 31:907–931
12. Everett WR, Rechnitz GA (1998) Mediated bioelectrocatalytic determination of organophosphorus pesticides with a tyrosinase-based oxygen biosensor. Anal Chem 70:807–810
13. Carralero V, Mena ML, Gonzalez-Cortes A, Yanez-Sedeno P, Pingarron JM (2006) Development of a high analytical performance-tyrosinase biosensor based on a composite graphite-Teflon electrode modified with gold nanoparticles. Biosens Bioelectron 22:730–736
14. Cosnier S, Szunerits S, Marks RS, Lellouche JP, Perie K (2001) Mediated electrochemical detection of catechol by tyrosinase-based poly(dicarbazole) electrodes. J Biochem Biophys Methods 50:65–77
15. Li X, Sun C (2005) Bioelectrochemical response of the polyaniline tyrosinase electrode to phenol. J Anal Chem 60:1073–1077
16. Kochana J, Gala A, Parczewski A, Adamski J (2008) Titania sol-gel-derived tyrosinase-based amperometric biosensor for determination of phenolic compounds in water samples. Examination of interference effects. Anal Bioanal Chem 391:1275–1281
17. Kim GY, Shim J, Kang MS, Moon SH (2008) Preparation of a highly sensitive enzyme electrode using gold nanoparticles for measurement of pesticides at the ppt level. J Environ Monit 10:632–637
18. Liu ZM, Liu J, Shen GL, Yu RQ (2006) A reagentless tyrosinase biosensor based on 1,6-hexanedithiol and nano-Au self-assembled monolayers. Electroanal 18:1572–1577
19. Moghaddam AB, Ganjali MR, Niasari M, Ahadi S (2008) Bioelectrocatalysis of dopamine using adsorbed tyrosinase on single-walled carbon nanotubes. Anal Lett 41:3161–3176
20. Zhou XQ, Yu T, Zhang YH, Kong JL, Tang Y, Marty JL, Liu BH (2007) Nanozeolite-assembled interface towards sensitive biosensing. Electrochem Commun 9:1525–1529

21. Wang S, Tan Y, Zhao D, Liu G (2008) Amperometric tyrosinase biosensor based on Fe3O4 nanoparticles-chitosan nanocomposite. Biosens Bioelectron 23:1781–1787
22. Sheldon RA (2007) Enzyme immobilization: the quest for optimum performance. Adv Synth Catal 349:1289–1307
23. Hanefeld U, Gardossi L, Magner E (2009) Understanding enzyme immobilisation. Chem Soc Rev 38:453–468
24. Adamski J, Nowak P, Kochana J (2010) Simple sensor for the determination of phenol and its derivatives in water based on enzyme tyrosinase. Electrochim Acta 55:2363–2367
25. Ismaya WT, Rozeboom HJ, Weijn A, Mes JJ, Fusetti F, Wichers HJ, Dijkstra BW (2011) Crystal structure of agaricus bisporus mushroom tyrosinase: identity of the tetramer subunits and interaction with tropolone. Biochemistry 50:5477–5486
26. Duckwort HW, Coleman JE (1970) Physicochemical and kinetic properties of mushroom tyrosinase. J Biol Chem 245:1613–1625
27. Wilcox DE, Porras AG, Hwang YT, Lerch K, Winkler ME, Solomon EI (1985) Substrate-analog binding to the coupled binuclear copper active-site in tyrosinase. J Am Chem Soc 107:4015–4027
28. Orenes-Pinero E, Garcia-Carmona F, Sanchez-Ferrer A (2006) Kinetic characterization of cresolase activity of *Streptomyces antibioticus* tyrosinase. Enzyme Microb Technol 39:158–163
29. Fenoll LG, Rodriguez-Lopez JN, Garcia-Sevilla F, Tudela J, Garcia-Ruiz PA, Varon R, Garcia-Canovas F (2000) Oxidation by mushroom tyrosinase of monophenols generating slightly unstable *o*-quinones. Eur J Biochem 267:5865–5878
30. Ros JR, Rodriguezlopez JN, Varon R, Garciacanovas F (1994) Kinetics study of the oxidation of 4-tert-butylphenol by tyrosinase. Eur J Biochem 222:449–452
31. Bard AJ, Faulkner LR (2001) Electrochemical methods: fundamentals and applications, 2nd edn. Wiley, New York
32. Michaelis L, Menten ML, Johnson KA, Goody RS (2011) The original Michaelis constant: translation of the 1913 Michaelis–Menten paper. Biochemistry 50:8264–8269
33. Lerch K, Ettlinge L (1972) Purification and characterization of a tyrosinase from Streptomyces-Glaucescens. Eur J Biochem 31: 427–437
34. Riley PA (2000) Tyrosinase kinetics: a semi-quantitative model of the mechanism of oxidation of monohydric and dihydric phenolic substrates. J Theor Biol 203:1–12
35. Fenoll LG, Rodriguez-Lopez JN, Garcia-Sevilla F, Garcia-Ruiz PA, Varon R, Garcia-Canovas F, Tudela J (2001) Analysis and interpretation of the action mechanism of mushroom tyrosinase on monophenols and diphenols generating highly unstable *o*-quinones. BBA-Protein Struct M 1548:1–22
36. Munoz JL, Garcia-Molina F, Varon R, Rodriguez-Lopez JN, Garcia-Canovas F, Tudela J (2006) Calculating molar absorptivities for quinones: application to the measurement of tyrosinase activity. Anal Biochem 351:128–138
37. Garciacarmona F, Garciacanovas F, Iborra JL, Lozano JA (1982) Kinetic-study of the pathway of melanization between L-dopa and dopachrome. Biochim Biophys Acta 717:124–131